Inorg. Chem. **1985**, *24*, 3271–3278

Contribution from the Department of Chemistry, Schlundt Hall,
University of Missouri, Columbia, Missouri 65201

Condensation of a Pseudoaromatic Planar Nickel(II) Complex: Structural and Kinetic Studies†

A. F. GHIRON, R. KENT MURMANN,* and E. O. SCHLEMPER

Received December 5, 1984

In dilute acid solution [Ni((PnAO)-6H)]^0, (2,2,3,9,10,10-hexamethyl-5,7-dioxa-6-hydra-1,4,8,11-tetraazacyclotetradeca-3,8,11,13-tetraene)nickel(II) (A), in its oxime-protonated form, [Ni((PnAO)-5H)]$^+$ (B), slowly converts to [Ni((PnAO)-7H)]$_2$(–CH–)$_3$]$^+$, [μ-[[3,3′-[[6-[[(1,1-dimethylacetonyl)amino]methylene]-2-[*N*-(1,1-dimethylacetonyl)formimidoyl]-2,4-heptadienediylidene]dinitrilo]bis[3-methyl-2-butanone] tetraoximato](3–)]]dinickel(1+) salt (C). C is a highly conjugated, deep purple ion with high kinetic stability. These studies imply that acid hydrolysis of the parent complex A produces $OHCCH_2CHO$, which in turn reacts with intact A to yield the dinickel complex C in two steps. This reaction has been modeled by the reaction of malondialdehyde and methylmalondialdehyde with A to produce C or its analogue. Spectral data, crystal structures of A, its protonated form B, and C, and some kinetic data are presented. [Ni((PnAO)-6H)]^0 (A) crystallizes in the monoclinic space group $P2_1/c$ with $a = 10.659$ (3) Å, $b = 10.097$ (4) Å, $c = 15.018$ (5) Å, $\beta = 101.96$ (2)°, $V = 1581$ (1) Å^3, and $Z = 4$ with final $R = 0.040$ and $R_w = 0.047$. [Ni((PnAO)-5H)]$^+ClO_4^-$ (B) crystallizes in the monoclinic space group $P2_1/c$ with $a = 10.268$ (1) Å, $b = 15.880$ (3) Å, $c = 11.452$ (2) Å, $\beta = 96.55$ (1)°, $V = 1855.2$ (9) Å^3, and $Z = 4$ with final $R = 0.035$ and $R_w = 0.051$. [[Ni((PnAO)-7H)]$_2$(–CH–)$_3$]$^+NO_3^-\cdot 2H_2O$ (C) crystallizes in the monoclinic space group $C2/c$ with $a = 22.374$ (5) Å, $b = 11.459$ (2) Å, $c = 14.573$ (6) Å, $\beta = 101.25$ (3), $V = 3664$ (3) Å^3, and $Z = 4$ with final $R = 0.026$ and $R_w = 0.034$.

Introduction

Some years ago it was found that the (2,2,3,9,10,10-hexamethyl-5,7-dioxa-6-hydra-1,4,8,11-tetraazacyclotetradeca-3,8-diene)nickel(II) ion, [Ni((PnAO)-H)]$^+$, was easily oxidized in basic solution to [Ni((PnAO)-6H)]^0, a quasi-aromatic system of unusual properties.[1–3] The neutral (2,2,3,9,10,10-hexamethyl-5,7-dioxa-6-hydra-1,4,8,11-tetraazacyclotetradeca-3,8,11,13-tetraene)nickel(II), [Ni((PnAO)-6H)]^0 (A), was easily prepared, but difficulty was encountered in obtaining single crystals for a structural study due to extensive twinning. Thus, structure determinations by X-ray diffraction were carried out on the C12–(NO)[4a] (Figure 2) and the C12–(NO$_2$)[4b] derivatives which established the planar nature of the complex and the distribution of unsaturation. Our continued interest in [Ni((PnAO)-6H)]^0 stems from the reactivity of the six-membered ring (3 C, 2 N, 1 Ni), which appears to be benzene-like with a high electron density on the center carbon, C12. Thus in many respects this ring behaves like a phenol or aromatic amine while the rest of the molecule remains unreactive. Similar reactivity has been suggested for other pseudoaromatic metal complexes.[5–8] This property has been used for attachment of functional groups and subsequent building of structures resembling biological molecules.[9]

In acidic media, the spectrum of [Ni((PnAO)-6H)]^0 changes slightly in a reversible manner,[2] suggesting protonation which probably occurs at the oxime hydrogen bond position to give compound B. It was presumed that this results in breaking the internal hydrogen bond, giving two N-coordinated oxime groups (see discussion of the structure later in this paper). Over a longer period of time or at elevated temperatures the pale orange-red color of the parent complex in acid solution changes irreversibly to deep purple. Crystalline salts of this product can be obtained by the addition of soluble salts of appropriate anions. The proton NMR spectrum of C was almost identical with that of the starting complex.[1,2] These studies report our efforts to understand the nature of these changes. It will be shown that the reactions involved may be summarized by the equations in Figure 1 in which a (–CH–)$_3$ group or –CHC(CH$_3$)CH– connects two parent [Ni((PnAO)-6H)]^0 complexes at the C12 positions in the purple nickel(II) dimer.

This reaction was particularly intriguing since other examples of self-condensation of tetraaza Ni macrocycles have resulted in direct coupling of the parent complexes and required either a redox reaction or long reaction time.[10,11]

Experimental Section

Instrumentation. The UV-vis spectra were recorded on Cary Models 12 and 14 instruments or a Beckman Model B spectrophotometer. The Model B had water-jacketed cells for temperature control, and the Model 14 had a temperature-controlled compartment. The ^{1}H and ^{13}C NMR spectra were taken on Varian EM360L and Nicolet-300 spectrometers. Computations for the kinetics were done with an Apple II+ microcomputer.[12,13]

Materials. [Ni((PnAO)-6H)]^0 was prepared by oxidizing [Ni((PnAO)-H)]ClO$_4$ with KIO$_3$ by the method of Vassian.[2] [Ni((PnAO)-H]ClO$_4$ was prepared in water solution by Vassian's method[2] from NiCl$_2$ and PnAO. Single crystals of [Ni((PnAO)-6H)] for X-ray analysis were obtained by the slow evaporation of acetonitrile solution while [Ni((PnAO)-5H)]ClO$_4$ crystals were obtained by cooling aqueous solutions of [Ni((PnAO)-6H)] that were also 1 M in HClO$_4$. It was recrystallized from water. Malondialdehyde bis(dimethyl acetal) and propionaldehyde diethyl acetal were obtained commercially. The sodium salt of 2-methylmalondialdehyde was prepared from the reaction of propionaldehyde diethyl acetal with dimethylformamide according to the method of Moschel and Leonard[14] as modified by Nair, Vietti, and Cooper.[15] The extinction coefficient was found to be 1.74 × 10^4 in 0.1 M H$^+$ at 250 nm (^{1}H NMR (D$_2$O, external Me$_4$Si in CH$_2$Cl$_2$): δ 8.48 (s, 2 H), 1.58 (s, 3 H)).

The sodium salt of malondialdehyde was prepared by the acid hydrolysis of malondialdehyde bis(dimethyl acetal) by the method of George and Mansell as modified by Nair, Vietti, and Cooper[15] (^{1}H NMR (D$_2$O, external Me$_4$Si in CH$_2$Cl$_2$): δ 8.70 (d, $J = 10.2$ Hz, 2 H) 5.3 (t, $J = 10.2$ Hz, 1 H)). The extinction coefficient at 245 nm is 1.02 × 10^4 in 0.01 M H$^+$, confirming that reported by Nair.[15] Due to the extreme instability of this salt we were unable to use it in accurate kinetic studies. The salt isolated always contained a small amount of polymeric material which rapidly reacted with the parent nickel complex, yielding a blue complex with an ϵ_{max} at 610–620 nm.

---

† A preliminary report of this work was presented at the American Crystallography Association meeting, Columbia, MO, March 1983.

(1) Urban, I. O.; Vassian, E. G. *Inorg. Chem.* **1979**, *18*, 867.
(2) Vassian, E. G.; Murmann, R. K. *Inorg. Chem.* **1967**, *6*, 2043.
(3) Hussain, M. S.; Schlemper, E. O. *Inorg. Chem.* **1979**, *18*, 2275.
(4) (a) Schlemper, E. O.; Murmann, R. K., unpublished work. (b) Hussain, M. S.; Murmann, R. K.; Schlemper, E. O. *Inorg. Chem.* **1980**, *19*, 1445.
(5) Hipp, C.; Busch, D. *Inorg. Chem.* **1973**, *12*, 894.
(6) Collman, J. P. "Reactions of Coordinated Ligands and Homogeneous Catalysis"; Gould, R. Ed.; American Chemical Society: Washington, DC, 1963; Adv. Chem. Ser. No. 37, p 78.
(7) Martin, J. A.; Wei, R. M. C.; Cummings, S. C. *Inorg. Chem.* **1972**, *11*, 475.
(8) Elfring, W., Jr.; Rose, N. *Inorg. Chem.* **1975**, *14*, 2759.
(9) Korybat-Daszkiewicz, B.; et al. *Inorg. Chem.* **1984**, *23*, 903.
(10) Cunningham, J.; Sievers, R. *J. Am. Chem. Soc.* **1973**, *95*, 7183.
(11) McElroy, G.; Dabrowiak, J. *J. Am. Chem. Soc.* **1976**, *98*, 7112. Switzer, J. A.; Endecott, J. F. *J. Am. Chem. Soc.* **1980**, *102*, 1181.
(12) "NLLSQ-Non Linear Least Squares for the Apple II"; CET Research, P.O. Box 2029, Norman, OK 73070.
(13) Ghiron, K. M. "A Runge-Kutta Method for Solving Simultaneous Differential Equations and Plotting and Filing Routines for the Apple II"; University of Missouri: Columbia, MO, 1984.
(14) Moschel, R. C.; Leonard, N. J. *J. Org. Chem.* **1976**, *41*, 294.
(15) Nair, V.; Vietti, D. E.; Cooper, C. S. *J. Am. Chem. Soc.* **1981**, *103*, 3030.

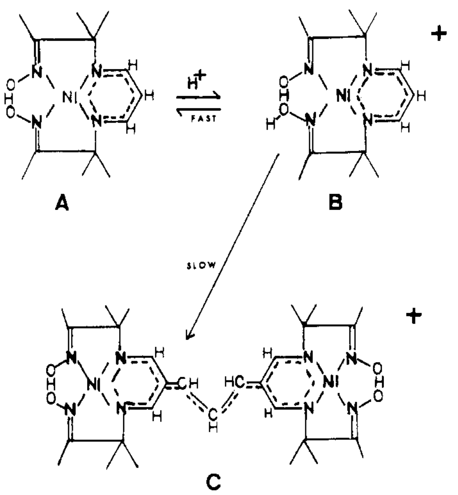

Figure 1. Reaction scheme for the formation of Ni-3C-Ni.

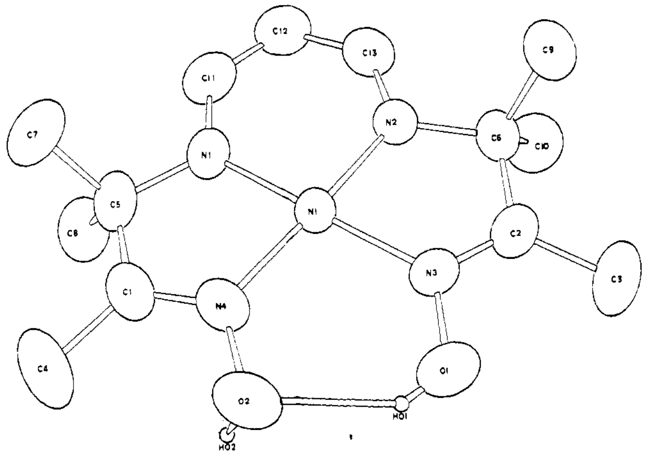

Figure 2. ORTEP drawing of $[Ni((PnAO)\text{-}5H)]^+$ with atom names.

Crystals of the binuclear bridged complexes (Ni-3C-Ni and Ni-4C-Ni) were prepared from solutions 3×10^{-3} M in the $[Ni((PnAO)\text{-}6H)]^0$, 1.5×10^{-3} M in the bridge dialdehyde, and 0.25 M in acid of the anion in question. Depending upon the anion used, reactions were allowed to occur for 2–4 days under N_2 and the crystals that separated were collected on a filter, washed with a small amount of acid solution, and dried. The crystals were generally of two forms, flat gold plates and deep purple needles, which appeared to be only different crystal habits. We were unable to form correctly sized and shaped crystals for a single-crystal X-ray study in this manner. The nitrate salt is more insoluble than the chloride while the perchlorate salt of the protonated $[Ni((PnAO)\text{-}6H)]^0$ is so insoluble that it was often deposited along with the perchlorate salt of Ni-3C-Ni. Crystals formed in this way were used for the ^1H and ^{13}C NMR studies and for the extinction coefficient determinations.

Crystals of the Ni-3C-Ni complex could also be formed by simply heating a small beaker containing a 0.25 M HCl solution with a high concentration of $[Ni((PnAO)\text{-}6H)]^0$. Crystals formed in this way had the same visible spectra and extinction coefficients as those prepared by the method above and the same ^1H NMR spectra as given by Vassian.[16] The X-ray structure of Ni-3C-Ni (C) was established on a single crystal produced in this way.

X-ray Structural Determination. For each compound (A–C) the following general procedure was followed. On the basis of 25 carefully centered reflections with Mo Kα radiation ($\lambda = 0.7107$ Å) arbitrarily selected by an Enraf-Nonius CAD4 diffractometer and from systematic absences, the unit cell parameters and space group were determined. Three-dimensional intensity data were collected at 21 °C, with use of Mo Kα radiation from a graphite monochromator and with use of the θ–2θ step scan technique. The intensities were measured with variable scan speeds to maintain counting statistics to 3% up to a maximum scan time of 120 s. Standard reflections were measured after every 6000 s of X-ray exposure and showed no decomposition over the period of measurement. Crystal orientation was maintained by checking the centering of the 3 reflections after the measurement of each 200 reflections and recentering as necessary. Empirical absorption correction factors from ψ scans ranged over less than 7% and averaged less than 3% in the worst case due to the small crystals and the low μ. No absorption corrections were made.

The structures were solved by conventional Patterson and Fourier methods. The full-matrix least-squares refinement minimized the function $\sum w(|F_o| - |F_c|)^2$, where $w = 1/(\sigma(F_o))^2$, $\sigma(F_o) = \sigma(F_o^2)/2F_o$, and $\sigma^2(F_o^2) = [\sigma^2_{count} + (0.03F_o^2)^2]$. Atomic scattering factors were taken from ref 17 and included anomalous scattering contributions. Hydrogen atoms were located from difference Fourier maps and were refined with fixed isotropic temperature factors. In structure B the perchlorate ion oxygens were partially disordered and a second set of four oxygens at 20% occupancy were found, which gave a good final fit to the data.

Reaction Kinetics. Stock solutions of the appropriate concentrations were prepared by dissolving $[Ni((PnAO)\text{-}6H)]^0$, malondialdehyde bis(dimethyl acetal) (MATA), and the sodium salt of methyl malondialdehyde (MMDA) in ethanol, methanol, and aqueous 0.05 M HCl, respectively. Bridge reaction solutions were prepared by mixing aliquots of the MATA or MMDA stock solutions with 0.01–0.5 M HCl whose ionic strength was adjusted when necessary with KCl. These solutions were flushed with and held under N_2 and equilibrated to the appropriate temperature before use. In the case of MATA they were allowed to stand about 12 h at 25 °C to ensure hydrolysis of the acetal to the dialdehyde (MDA) (required 3 h in 0.25 M H^+ and at 25 °C). The reaction was started by mixing a 25-μL aliquot of the $[Ni((PnAO)\text{-}6H)]^0$ stock with the bridging solution and stirring with N_2. Samples were sealed under N_2 in a cuvette and placed in a temperature-controlled water bath, and the optical density was obtained periodically. For slow reactions the reaction vessel, approximately 50 mL, was sealed under N_2 and held in a constant-temperature water bath and samples were removed periodically for spectrophotometric readings. A N_2 atmosphere was constantly maintained over all solutions.

The appearance of the MDA "intermediate" was monitored at 390 nm, the MMDA "intermediate" at 380 nm, and both Ni-3C-Ni and Ni-4C-Ni at 548 nm.

For studies on the rate of formation of the intermediates, excess MDA and MMDA were present. The first step was then pseudo first order in $[Ni((PnAO)\text{-}6H)]^0$, and the second step, formation of Ni-3C-Ni or Ni-4C-Ni, was prevented by the 20-fold excess of MDA. A lower ratio led to the formation of some C and more led to the appearance of a new substance (ϵ_{max} at 610–620 nm). The latter is believed to result from the reaction of A with traces of some condensed MDA species. A 40-fold excess of MMDA was found to be satisfactory to accomplish the same objectives with this aldehyde. The rate measurements on the intermediates were generally followed for 4 half-lives and the infinity readings predicted by an exponential fit of the data with the program NLLSQ.[12] The infinity values were always checked with a measured value under comparable conditions. The rate of the reaction was lowered by the presence of oxygen, and care had to be taken to keep contact with traces of air to the minimum. The observed first-order rate constants, k_{obsd}, were calculated from the slopes of the linear plots of ln $(A_\infty - A)/(A_\infty - A_0)$ vs. t.

During preliminary studies, the initial rates of formation of the product C were determined by following the absorbance of 548 nm for the first 10% of the reaction, when near-stoichiometric amounts of the dialdehyde were present. Infinite values were determined after 2 days with MDA and 4 days with MMDA. Progress of the reaction was also followed spectrally in order to compare with infinity values calculated. The calculations were for two sequential reactions and used the Runge–Kutta method.[13] In the calculations the experimentally determined values of the extinction coefficients of B and C and the second-order rate constant of the first step were used, allowing a determination of the limits of the rate constant for the second step and also an estimate of the rate of the breakdown of $[Ni((PnAO)\text{-}6H)]^0$, k_0, to form MDA. k_0 was also obtained from the linear portion of the d[B]/dt curve after a steady state had been achieved.

Results

The crystal structure determination parameters are given in Table I for the three compounds reported in this work, and the positional parameters of the atoms with their estimated errors are in Table II. Figure 2 is an ORTEP drawing of the protonated parent molecule ion B with the naming system (the same for all three complexes). $[Ni((PnAO)\text{-}6H)]^0$ has exactly the same molecular structure but without the outside H atom (HO2) on

---

(16) Vassian, E. G. Ph.D. Thesis, University of Missouri, Columbia, MO, 1967.

(17) "International Tables for X-ray Crystallography"; Kynoch Press: Birmingham, England, 1974; Vol. IV.

Table I. Crystal Data Collection Parameters

	$[Ni((PnAO)\text{-}6H)]^0$	$[Ni((PnAO)\text{-}5H)]^+ClO_4^-$	$[Ni((PnAO)\text{-}7H)_2(\text{–}CH\text{–})_3]^+\cdot 2H_2O$
formula	$NiO_2N_4C_{13}H_{22}$	$NiClO_6N_4C_{13}H_{23}$	$Ni_2O_9N_9C_{29}H_{49}$
fw	325.06	425.15	785.20
space group	$P2_1/c$	$P2_1/c$	$C2/c$
a, Å	10.659 (3)	10.268 (1)	22.374 (5)
b, Å	10.097 (4)	15.880 (3)	11.459 (2)
c, Å	15.018 (5)	11.452 (2)	14.573 (6)
β, deg	101.96 (2)	96.55 (1)	101.25 (3)
V, A^3	1581 (1)	1855.2 (9)	3664 (3)
Z	4	4	4
D_{calcd}, D_{obsd}, g/cm^3	1.365, 1.38	1.522, 1.50	1.423, 1.39
μ, cm^{-1}	12.4	14.0	10.9
no. of reflcns measd	1679	4678	3509
no. of reflcns above 1.5σ	1481	4014	2616
no. of indep reflcns	1116	2411	1657
no. of atoms	42	48	51
no. of variables	247	295	296
no. of indep observns above 1.5σ	1092	2043	1271
$R(F_o) = \sum \lVert F_o\vert - \vert F_c\vert / \sum F_o$	0.040	0.035	0.026
$R_w(F_o) = [\sum w(F_o - F_c)^2/\sum wF_o^2]^{1/2}$	0.047	0.051	0.034
max shift/error on last cycle	0.15	0.21	0.10
error in observn of unit wt	1.30	1.66	1.05

Table II. Positional Parameters (Standard Deviations in Parentheses) of $[Ni((PnAO)\text{-}6H)]^0$ (A), $[Ni((PnAO)\text{-}5H)]ClO_4$ (B), and $[Ni\text{-}3C\text{-}Ni]NO_3$ (C)

A				B				C			
atom	*x*	*y*	*z*	atom	*x*	*y*	*z*	atom	*x*	*y*	*z*
Ni	0.24783 (8)	0.05077 (9)	0.19822 (5)	Ni	−0.47918 (4)	−0.15900 (2)	−0.11121 (3)	Ni	−0.13596 (2)	0.10369 (5)	0.37602 (3)
O(1)	0.2973 (5)	0.9768 (6)	0.3845 (3)	Cl	0.1473 (1)	0.01172 (7)	0.2899 (1)	O(1)	−0.1879 (1)	0.0377 (3)	0.1877 (2)
O(2)	0.1482 (5)	0.3445 (5)	0.8439 (3)	O(1)	−0.3682 (3)	0.0086 (2)	−0.0752 (3)	O(2)	−0.1757 (1)	0.2447 (3)	0.2160 (2)
N(1)	0.1819 (5)	0.1530 (5)	0.0976 (3)	O(2)	−0.5719 (3)	−0.0043 (2)	−0.2332 (3)	O(3)	−0.0477 (2)	0.3797 (3)	0.7207 (3)
N(2)	0.6592 (5)	0.0623 (6)	0.8583 (3)	O(3)	0.2766 (4)	0.0173 (2)	0.3483 (4)	O(4)	0.0000 (0)	0.5382 (4)	0.7500 (0)
N(3)	0.6810 (5)	0.0504 (6)	0.7000 (3)	O(4)	0.1624 (4)	−0.0453 (2)	0.1850 (3)	O(5)	−0.0765 (2)	−0.3046 (4)	0.6326 (3)
N(4)	0.1507 (5)	0.1646 (6)	0.2543 (3)	O(5)	0.0648 (4)	−0.0367 (3)	0.3556 (4)	N(1)	−0.1055 (1)	0.2022 (3)	0.4753 (2)
C(1)	0.0854 (7)	0.2569 (7)	0.2074 (5)	O(6)	0.0881 (5)	0.0829 (3)	0.2440 (5)	N(2)	−0.1197 (1)	−0.0328 (3)	0.4422 (2)
C(2)	0.6093 (7)	0.1468 (7)	0.7089 (5)	N(1)	−0.5951 (3)	−0.2409 (2)	−0.1693 (2)	N(3)	−0.1667 (1)	0.0028 (3)	0.2777 (2)
C(3)	0.554 (1)	0.269 (1)	0.1282 (7)	N(2)	−0.3738 (3)	−0.2289 (2)	−0.0142 (2)	N(4)	−0.1525 (1)	0.2419 (3)	0.3097 (2)
C(4)	0.0061 (9)	0.147 (1)	0.7469 (6)	N(3)	−0.3584 (3)	−0.0780 (2)	−0.0474 (3)	N(5)	0.0000 (0)	0.4322 (4)	0.7500 (0)
C(5)	0.0942 (6)	0.2591 (7)	0.1086 (4)	N(4)	−0.5873 (3)	−0.0909 (2)	−0.2155 (3)	C(1)	−0.1431 (2)	0.3389 (4)	0.3533 (3)
C(6)	0.5911 (7)	0.1717 (7)	0.8031 (5)	C(1)	−0.6848 (3)	−0.1233 (2)	−0.2802 (3)	C(2)	−0.1661 (2)	−0.1074 (4)	0.2934 (3)
C(7)	0.1446 (9)	0.1070 (8)	0.5872 (5)	C(2)	−0.2626 (3)	−0.0992 (2)	0.0276 (3)	C(3)	−0.1869 (2)	−0.1959 (4)	0.2195 (3)
C(8)	0.9604 (8)	0.265 (1)	0.5511 (6)	C(3)	−0.1305 (4)	−0.2276 (3)	0.0194 (4)	C(4)	−0.1575 (2)	0.4539 (4)	0.3073 (3)
C(9)	0.4485 (7)	0.1728 (9)	0.8041 (5)	C(4)	−0.7056 (5)	−0.2640 (3)	−0.3704 (3)	C(5)	−0.1160 (2)	0.3292 (4)	0.4558 (3)
C(10)	0.6536 (9)	0.3058 (8)	0.8368 (7)	C(5)	−0.7057 (3)	−0.2150 (2)	−0.2559 (3)	C(6)	−0.1431 (2)	−0.1426 (4)	0.3934 (3)
C(11)	0.2112 (7)	0.1345 (8)	0.0160 (4)	C(6)	−0.2579 (3)	−0.1912 (3)	0.0559 (3)	C(7)	−0.0555 (2)	0.3974 (4)	0.4763 (3)
C(12)	0.2905 (7)	0.0380 (8)	0.9955 (4)	C(7)	−0.7722 (4)	−0.0739 (3)	−0.3677 (3)	C(8)	−0.1598 (2)	0.3767 (4)	0.5153 (3)
C(13)	0.6486 (7)	0.0544 (8)	0.9443 (5)	C(8)	−0.8359 (4)	−0.2238 (3)	−0.2039 (3)	C(9)	−0.1960 (2)	−0.1886 (4)	0.4356 (3)
HOO	0.774 (5)	0.553 (7)	0.135 (4)	C(9)	−0.1620 (4)	−0.0384 (3)	0.0809 (4)	C(10)	−0.0927 (2)	−0.2335 (4)	0.4003 (3)
				C(10)	−0.2642 (5)	−0.2026 (3)	0.1884 (4)	C(11)	−0.0761 (2)	0.1703 (4)	0.5576 (3)
				C(11)	−0.5888 (4)	−0.3209 (2)	−0.1393 (3)	C(12)	−0.0650 (2)	0.0517 (4)	0.5860 (3)
				C(12)	−0.4937 (4)	−0.3565 (2)	−0.0604 (4)	C(13)	−0.0892 (2)	−0.0421 (4)	0.5274 (3)
				C(13)	−0.3919 (4)	−0.3118 (2)	−0.0034 (3)	C(14)	−0.0309 (2)	0.0193 (4)	0.6742 (3)
				HO1	−0.322 (3)	−0.001 (2)	−0.103 (3)	C(15)	0.0000 (0)	0.0826 (5)	0.7500 (0)
				HO2	−0.511 (3)	0.013 (2)	−0.207 (3)	HOO	−0.185 (2)	0.127 (4)	0.191 (3)

Table III. Selected Bond Angles (deg) and Their Standard Deviations

angle	$[Ni((PnAO)\text{-}6H)]^0$	$[Ni((PnAO)\text{-}5H)]^+$	Ni-3C-Ni
N1-Ni-N4	82.7 (3)	82.3 (1)	83.8 (2)
N1-Ni-N2	96.9 (3)	96.0 (1)	96.0 (2)
N3-Ni-N4	97.9 (3)	99.8 (1)	97.1 (2)
N1-C5-C1	106.0 (5)	106.2 (3)	106.2 (4)
N3-C2-C5	115.6 (6)	114.0 (3)	115.2 (4)
N1-C11-C12	125.3 (7)	125.4 (3)	124.2 (4)
C11-C12-C14			123.2 (4)
C12-C14-C15			133.2 (5)

the oxime oxygen. Figure 3 contains a similar drawing of the binuclear complex with some important distances and estimated errors. Other distances may be found in Figure 11. Table III has selected bond angles for the three compounds while Table IV contains selected planes and the deviations of the atom centers from those planes. Figure 4 shows the light absorption behavior of the three compounds in the region 2200–6700 Å.

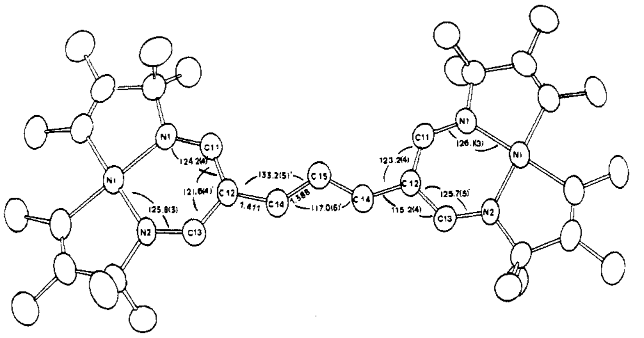

Figure 3. ORTEP drawing of Ni-3C-Ni with some bond angles and distances (distances ±0.005 Å).

In preliminary studies on the slow reaction of $[Ni((PnAO)\text{-}6H)]^0$ with dilute HNO_3, $HClO_4$, or HCl (0.1–0.5 M), it was found that the protonated complex B changes to the binuclear

Table IV. Least-Squares Planes[a]

		A	*B*	*C*	*D*
[Ni((PnAO)-6H)]^0	plane 1: Ni, N1, N2, N3, N4, O1, O2 (9, −44, 28, 13, 17, −50, 28)	−0.7474	−0.6311	−0.2076	2.4503
	other atoms: C1, C2, C5, C6 (66, −17, 145, −30)				
	plane 2: C11, C12, C13, N1, N2, Ni (−86, −32, −106, 32, 57, 134)	−0.7747	−0.6131	−0.1550	−2.4684
	dihedral angle: plane 1/plane 2 = 3.5°				
[Ni((PnAO)-5H)]ClO$_4$	plane 1: Ni, N1, N2, N3, N4 (−8, −16, 20, −15, 19)	0.6560	−0.1845	−0.7319	−1.7323
	other atoms: O1, O2, C1, C2, C5, C6 (−61, 40, −5, 58, 47, −42)				
	plane 2: Ni, N1, N2, C11, C12, C13 (−2, −8, 12, 6, −6, −2)	0.6432	−0.1786	−0.7446	−1.6770
	dihedral angle: plane 1/plane 2 = 1.1°				
Ni-3C-Ni	plane 1: Ni, N1, N2, N3, N4 (3, −2, 1, −2, 1)	0.9686	−0.0382	−0.2456	−5.3505
	other atoms: C1, C2, C5, C6 (−111, −41, 10, −187)				
	plane 2: C11, C12, C13, Ni, N1, N2 (−9, 50, −13, 58, −44, −42)	0.9473	−0.0231	−0.3197	−5.6975
	other atoms: C14, C15 (143, 229)				
	plane 3: Ni, N1, N2, N3, N4, Cl, C2, C5, C6, C11, C13 (−35, 27, 39, −86, −104, 29, −17, 150, 173, −40, −112, −25)	0.9954	−0.0231	−0.2944	−4.8141
	other atoms: C14, C15 (−239, −358)				
	plane 4: Ni′, N1′, N2′, C11′, C12′, C13′ (−58, 43, 42, 10, −50, 12)	0.9472	−0.0229	−0.3199	−5.1990
	dihedral angles: plane 1/plane 2 = 5.6°; plane 2/plane 4 = 2.6°; plane 1/C12,C14,C15 = 8.4°				

[a] The equation of the planes is of the form $Ax + By + Cz - D = 0$, where *A–D* are constants and *x–z* are orthogonalized coordinates. Respective deviations from the plane (10^3 Å) are given in parentheses (average esd 0.004 Å).

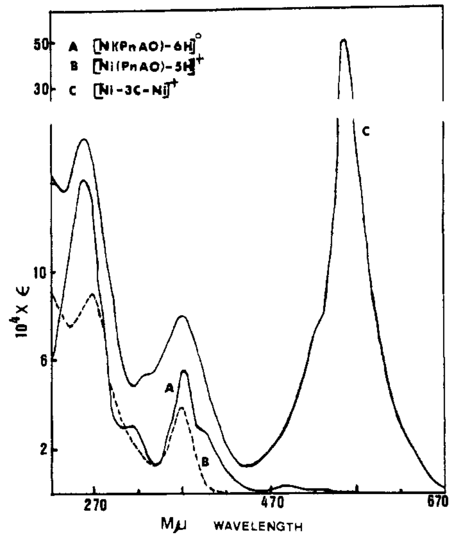

Figure 4. Absorption spectra of A–C.

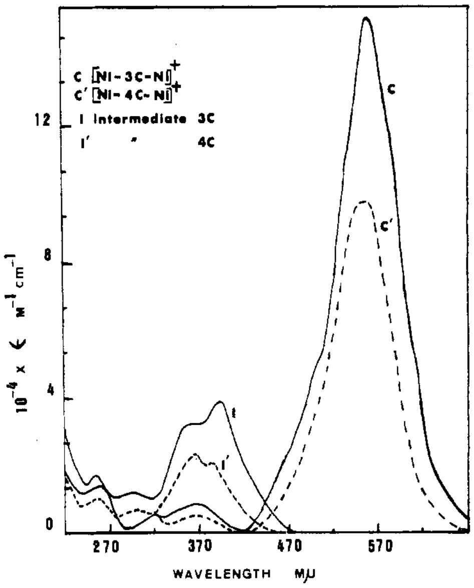

Figure 5. Absorption spectra of Ni-3C-Ni (C), Ni-4C-Ni (C′), and their respective intermediates.

complex C and an additional yellow nickel complex ion is also formed. The last complex is easily separated and observed by paper chromatography using 2-butanol–HCl solutions for separation. The yellow ion is unstable in acidic media, a characteristic of [Ni((AO)$_2$-H)]$^+$, the expected byproduct. It is tentatively concluded that C–N hydrolysis occurs on B, leading to malondialdehyde and [Ni((AO)$_2$-H)]$^+$. The latter ion dissociates rapidly in acidic media. The malondialdehyde then condenses with the remaining B at a rate faster than the hydrolysis, giving the final product C. When the reaction is conducted under an argon atmosphere, the yield of C is at least 80% of that expected. Since B and C are stable in oxygen but the overall reaction is affected by it, one or more of the intermediates leading to Ni-3C-Ni must be oxygen sensitive.

To establish that the -3C- group was generated by hydrolysis of [Ni((PnAO)-5H)]$^+$ and that malondialdehyde was the likely reactive product of the initial step, 2-methylmalondialdehyde (MMDA) was reacted with B under the same conditions. While the reaction was slightly slower than the MDA, a product was observed in solution and in the solid state with characteristics very similar to (but different from) those of Ni-3C-Ni. The spectrum of this product, Ni-4C-Ni, is compared with that of Ni-3C-Ni in Figure 5.

A study of the spectral changes with time for the reaction of A with MDA and MMDA showed than an intermediate (I) was formed, reached a maximum concentration, and then decreased as C was formed. The changes in absorbance where I has its maximum absorbance were very sensitive to the initial ratio of A/MDA as well as to the absolute concentrations because of the nature of sequential second-order reactions. Changes in concentration as a function of time for the dialdehyde, I, and C at one set of conditions is shown in Figure 6, and changes in ab-

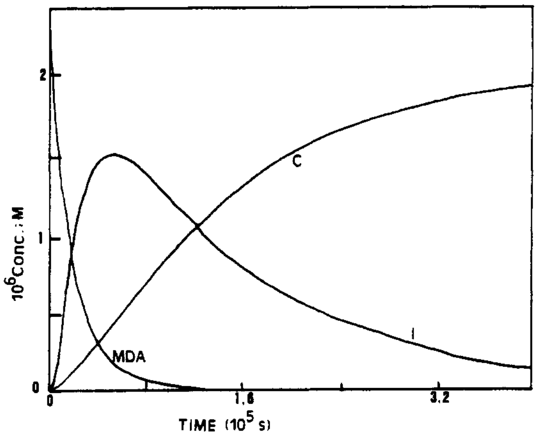

Figure 6. Runge–Kutta concentration vs. time graph for the reaction of A with MDA at 0.25 M H$^+$ and 25 °C ($[A]_0 = 2 \times 10^{-4}$ M, $[MDA]_0 = 1 \times 10^{-5}$ M).

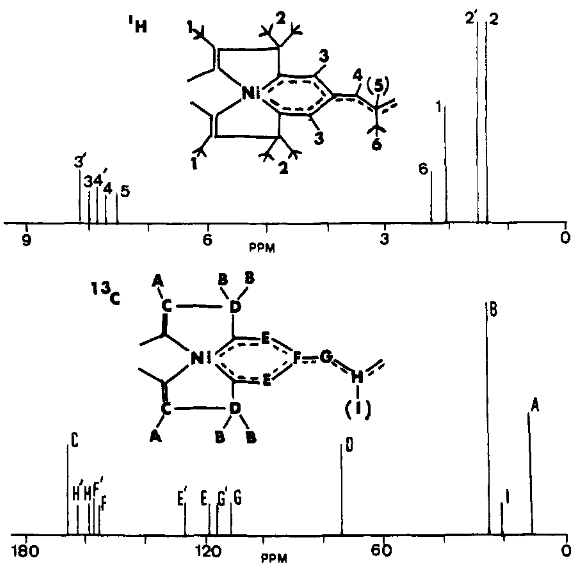

Figure 7. ^{13}C and ^{1}H NMR spectra of Ni-3C-Ni and Ni-4C-Ni (prime). When analogous peaks were at the same position for both compounds, the prime was not included. The height is equal to the approximate intensity of all split peaks attributed to that atom.

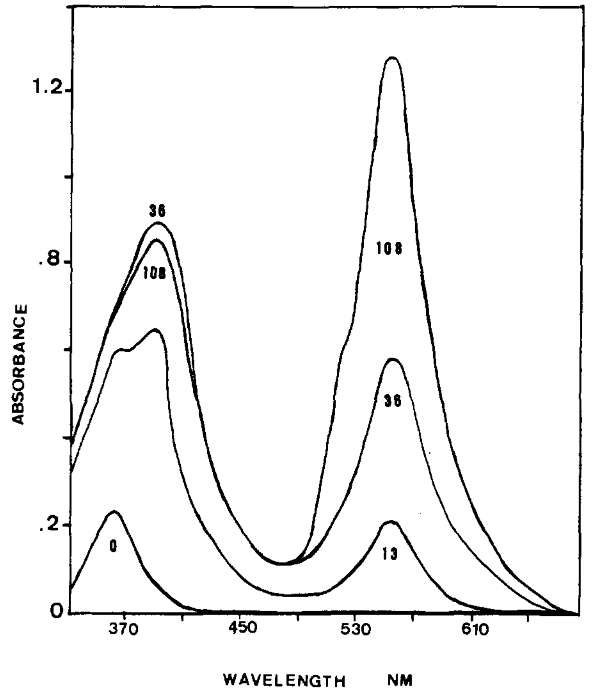

Figure 8. Absorption spectral changes of A + MDA at 25 °C and 0.25 M H^+ ($[A]_0 = 6.3 \times 10^{-5}$ M, $[MDA]_0 = 3.1 \times 10^{-5}$ M). Numbers refer to the time in hours.

sorbance with time are shown in Figure 8 for another set of conditions. The concentration vs. time curve was generated by a Runge–Kutta program using the experimentally determined k_1 and an optimized k_2 value for the best fit to the experimental absorbance data. The fit obtained was almost as good as that shown in Figure 12, which, however, contains the additional term k_0. The intermediate was separated by LC, and its spectrum was similar to that obtained in the 3C system (Figure 5). The proton and ^{13}C NMR spectra confirmed that the final product of the reaction with MMDA was analogous to that from MDA and showed the additional methyl resonance expected (Figure 7). At the time of writing, the crystals of this material, thin plates and thin needles, have not been suitable for X-ray study.

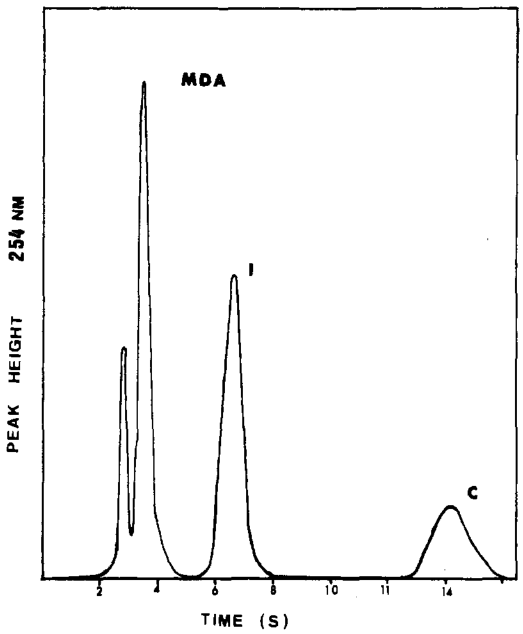

Figure 9. Liquid chromatographic separation of a mixture of reactants and products showing the separation of I. The first peak is the solvent front.

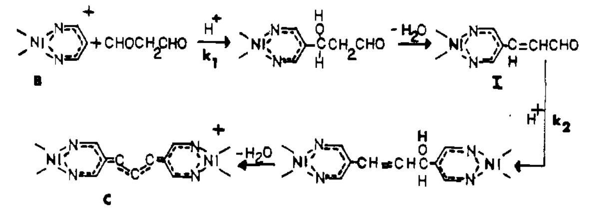

Figure 10. Reaction scheme showing the formation of the intermediates.

When stoichiometric amounts of $CHOCH_2CHO$ are reacted with $[Ni((PnAO)\text{-}6H)]^0$ in aqueous acid under argon, the same product (C) is produced in higher yields and under milder conditions. Figure 8 shows the spectral changes that occur with time with a 2/1 mole ratio of A/$CHOCH_2CHO$ in 0.25 M HCl at 25 °C. From these changes it is again clear that at least two sequential reactions are occurring. The first reaction leads to the formation of an intermediate (I) of unknown composition, which is most probably the condensation–dehydration product of B with one end of the dialdehyde. The second step could then be the condensation–dehydration reaction of another B with the free end of the dialdehyde attached to I. This intermediate has a distinct spectrum with a strong absorption band at 3850 Å. It was possible to separate this species from the others by liquid chromatography on a 30-cm C18 Bondpak column with a 60% methanol–40% water mobile phase (Figure 9) and to obtain its spectrum on a dynamic computer-controlled LC apparatus. The spectrum is given in Figure 6. It can also be separated from Ni-3C-Ni and excess reactants by benzene extraction, but a single extraction is not quantitative. From experiments at high and low dialdehyde/B ratios it was tentatively concluded that the reaction rates for the two steps were of the same order of magnitude.

Because of its extreme reactivity, malondialdehyde was added as the tetramethyl acetal in most of these studies and hydrolyzed to the dialdehyde by acid in situ. The free aldehyde prepared in this way appeared to be stable for 3 days at 25 °C when held under N_2. Malondialdehyde tends to condense on itself in neutral or basic media, producing materials that also react with B. We were unable to prepare disodium malonate pure enough to use in high aldehyde ratio studies since then some of the secondary product was always observed.

We have concluded that aside from the initial hydrolysis of $[Ni((PnAO)\text{-}6H)]^0$ the reactions are the same whether the dialdehyde is added to the reaction or not. Also only one intermediate is present in major amounts during the reaction. While we have not structurally characterized I, a reasonable case can be made for the reaction proceeding as shown in Figure 10.

Table V. Rate Constants in the Reaction of $[Ni((PnAO)\text{-}6H)]^0$ [a]

temp, °C	$[H^+]$, M	Ni-3C-Ni k_0	Ni-3C-Ni k_1	Ni-3C-Ni k_2	Ni-4C-Ni k_0	Ni-4C-Ni k_1	Ni-4C-Ni k_2
25	0.25	3×10^{-8}	0.274	0.035			
25	0.10	2×10^{-8}	0.190	0.032			
35	0.25	1.3×10^{-7}	0.430		1.3×10^{-7}	0.073	0.025

[a] Legend: k_0 = rate constant for the hydrolysis of B, in s^{-1}; k_1 = rate constant for B + dialdehyde → I, in $M^{-1}\ s^{-1}$; k_2 = rate constant for I + B → C, in $M^{-1}\ s^{-1}$. K_a = acid dissociation constant of $[Ni((PnAO)\text{-}5H)]^+$ at 25 °C ($A + H^+ \rightleftharpoons B$) = 0.08 M; ionic strength (KCl) = 0.5. Error estimates: k_0, ±30%; k_1, ±5.0%; k_2, ±15%.

One would anticipate significant spectral changes upon dehydration of either of the two alcohols formed by the aldehyde condensations, and thus four intermediates could have been observed (Figure 10). Only one intermediate is present in any appreciable amount. We know from the X-ray structure of C that it is in the completely dehydrated form, but no direct evidence is available about the intermediate. We suggest that it is likely that both dehydrations are rapid (compared to the other steps) due to the thermodynamic stability of the highly conjugated product. Similar purely organic dehydrations have been shown to be rapid, but we are unaware of a case analogous to that described here.

The results of kinetic studies on these two reactions show that the formation of the intermediate follows the rate law $-d[A]/dt = k_1[[Ni((PnAO)\text{-}5H)]^+][\text{aldehyde}]$ with a small positive acid dependency while the second step has the form $d[C]/dt = k_2[I][[Ni((PnAO)\text{-}5H)]^+]$ again with a small positive acid dependency. Table V gives some selected data establishing the conclusions stated for the first step and giving a few measurements on the second reaction. Separation of the two rate terms and accurate measurement was difficult because of spectral overlap and because the rates and rate constants are of similar magnitude. It is clear however that the second step is slower than the first by a factor of about 8, larger than the expected statistical factor. In reactions where the MDA/A ratio is close to unity the maximum [I] and the final [C] are closely related to k_1/k_2 as is the time of maximum [I].

Discussion

The primary objectives of the single-crystal X-ray studies were to exactly determine the structures of the starting materials and product, to identify the position of protonation of the primary reactant, and to ascertain the nature of the bonding in the complex portion of the product and in the $-(CH)_3-$ bridge.

The structure of A was difficult to determine because the crystals were nearly all twinned no matter what solvent was used for crystallization. Finally some single crystals were obtained, but these were smaller than desired and resulted in a smaller than optimal number of observations. However, with the high precision of the data (3%), satisfactory agreement factors and standard deviations were obtained. As shown in Figure 2, protonation of A takes place at an oxygen of the hydrogen-bonded oxime group but in a manner quite different than expected. The hydrogen atoms were located with reasonable certainty in this determination even though only X-ray data were used. The distances to hydrogen atoms are probably 0.1–0.2 Å shorter than actual, a characteristic of X-ray data. We expected the –O–H–O– bond to be broken and two –N–O–H bonds formed. However, it was found that –O–H–O protonation occurs, retaining a highly unsymmetrical

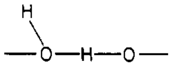

bond, and both the N–O and O–O bond distances increase in length (0.05–0.20 Å, respectively, Figure 11). While other forms of the protonated complex may be as stable or more stable in solution, this structure has considerably more stability than previously anticipated.

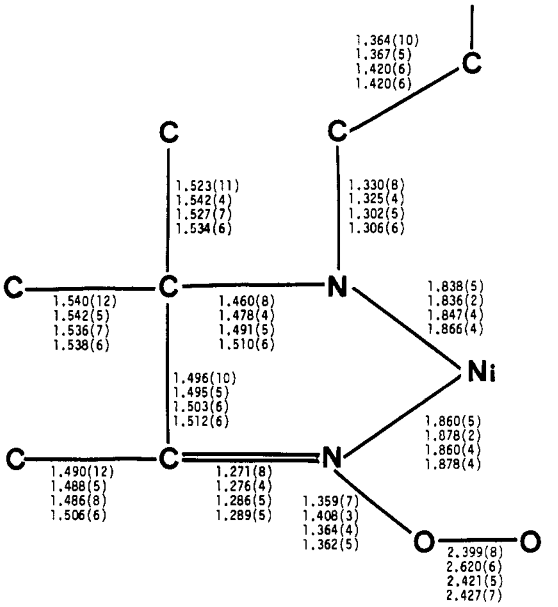

Figure 11. Bond distances from X-ray structures (averaged where there are two analogous positions) for (top to bottom) A, B, C, and $[Ni((PnAO)\text{-}7H)NO_2]^0$.[4b]

A further consideration of Figure 11 shows that all C–C and C–N distances in the aliphatic portions of the four structures are constant to within 2σ. Significant C–C differences do exist within a molecule with

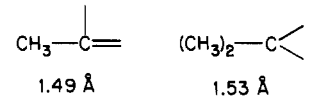

The bond distances within the (Ni,N_2,C_3) aromatic ring are shorter and more variable than in other parts of the molecule. Within that ring the C–C and C–N distances are shortened by about 0.16 and 0.17 Å, respectively, compared to normal single-bond distances. A very significant change occurs in the Ni–N bond distances. In a normal aliphatic α-amine oxime complex of Ni(II)[18,19] the nickel to N_{amine} distance is greater (by 0.03–0.07 Å) than that to N_{oxime}, but in all oxidized Ni(II) systems (those with a heterocyclic aromatic ring) the opposite is true; $Ni\text{–}N_{\text{oxime(av)}} = 1.869$ Å, $Ni\text{–}N_{\text{amine(av)}} = 1.844$ Å, and $\Delta = 0.025$ Å with the average deviation from the mean being about 0.004 Å. We interpret this in terms of delocalized multiple bonding among the atoms of the heterocyclic ring. In the two C12-substituted complexes there is evidence for conjugation of the aromatic ring to the substituent (–CHCHCH– or $-NO_2$) group resulting in significantly shortened ring C–N bonds and longer C–C and Ni–N bonds. For comparison the C–N bond in the aliphatic portion averages 1.485 Å while the C—N bond in the ring averages 1.316 Å and the C=N bond averages 1.281 Å.

Related to this, the C–C bond in the aromatic portion averages 1.393 Å compared to a C–C aliphatic average of 1.502 Å, also indicating double-bond character. The C–C distances in the C_3 bridging group of C are C12–C14 = 1.411 (6) Å and C14–C15 = 1.388 (6) Å and also show considerable double-bond character. Thus in this compound we apparently have significant conjugation through all of the atoms shown in Figure 1C. The C_3 bridge group is not linear with a C12–C14–C15 angle of 133.2 (5)° (Figure 3). The plane of the C_3 group is nearly coplanar with the halves of the dinuclear complex (see Table IV), again suggesting that considerable multiple bonding exists connecting the two complex ions. The bond angles within the complex ion vary only slightly between the three complexes studied (Table III). There is a significant increase in the N3–Ni–N4 bond angle upon protonation of an oxime oxygen. Apparently this is associated with the

---

(18) Schlemper, E. O. *Inorg. Chem.* **1968**, *7*, 1130–1135.

(19) Fair, C. K.; Schlemper, E. O. *Acta Crystallogr., Sect. B: Struct. Crystallogr. Cryst. Chem.* **1978**, *B34*, 436–442.

weakening of the O–H–O hydrogen bond, but only small changes occur in the other angles around Ni. The C12–C14–C15 angle, 133.2°, is far from linear or trigonal planar and is in line with multiple bonding between the bridging atoms and the ring. The angles in the pseudoaromatic ring are slightly over 120°, C11–C12–C13 = 121.6 (4)°, as are the ring to the bridge angles, C11–C12–C14 = 123.2(4)°, suggesting conjugation between these atoms.

The high planarity of these complexes is unique. Aside from the terminal methyl groups and the hydrogen atoms, all atoms of the complexes are in a reasonable plane. In complex A for example (Table IV) the Ni,N1,N2,N3,N4,O1,O2 plane contains those atoms to within 0.05 Å and C1,C2,C5,C6 to within 0.145 Å. The second plane calculated, C11,C12,C13,Ni,N2,Ni, contains all of its atoms to within 0.134 Å and makes a dihedral angle with the first plane of 3.5°.

Complex B, the protonated form, appears to have some of the strain caused by the hydrogen bond relieved, and planes similar to those given above show even less deviation from planarity, 0.07 Å being the maximum deviation.

The binuclear complex C is also very planar with only C1 and C6 deviating significant (0.187 Å) from the Ni,N1,N2,N3,N4 plane. Plane 2, containing the aromatic ring, has atoms only 0.05 Å out of the plane, but the bridging atoms, C14 and C15, are considerably outside of it: 0.143 and 0.229 Å. Plane 3 also shows the deviation of C14 and C15 from the plane containing all heavy atoms except the methyl groups. The dihedral angle between the Ni,N1,N2,N3,N4 plane and the plane described by the C12,C14,C15 atoms is 8.4°, a rather small value considering the potential flexibility of the bridging group.

From such considerations it is reasonable to describe the product ion C as planar and to say that the essential planarity of both metal complex segments and the bridging group in C is consistent with a conjugated system connecting metal ion centers through the bridging -3C- group and the quasi-aromatic rings as also suggested by the short bond distances.

The intramolecular hydrogen bond appears to be unaffected by substitution at the C12 position (Figure 11). The O–O bond length increases slightly by about 0.02 Å. The H atom is essentially symmetrically placed between the oxygen atoms within the estimated error. Protonation of the complex results in a 0.2-Å separation of the oxygens. HO1 is unsymmetrically situated (0.72, 1.98 Å) between O1 and O2 while HO2 is 0.62 Å from O1 and is also hydrogen bonded to the perchlorate oxygens O4 and O9 (2.64 and 2.69 Å, respectively). Thus protonation results in each hydrogen atom having a short bond to oxygen (about 0.7 Å) and a longer bond to either the other oxime oxygen or perchlorate oxygens (2.0, 2.6 Å).

Thus we have demonstrated that the decomposition of A in acid media gives malondialdehyde and $[Ni((AO)_2\text{-}H)]^+$ in the slowest step, k_0, and that the dialdehyde reacts more rapidly with the A remaining to give the conjugated binuclear species C in two steps. The first step produces an intermediate I, which has been separated by LC and isolated by benzene extraction and reacts with A to give C. Other active monoaldehydes such as CH_3CHO, C_6H_5CHO, and CF_3CHO react to form compounds analogous to I and have similar spectra but do not react further. One of these products, with CF_3CHO being used, has been isolated and its structure determined by NMR and will be reported in detail in a subsequent paper. The exact structure of I is not known in that the stage at which dehydration to the olefin takes place has not been determined. All evidence points to a single intermediate with both MDA and its methyl analogue MMDA.

The kinetics of the reactions were followed by measuring the rate of formation of I and C with A and MDA or MMDA as reactants. Both the formation of I and its subsequent reaction to form C were independently followed. It was found that only the protonated form of A, i.e. B, was reactive and that the rate law was $d[I]/dt = k_1[B][MDA]$. From the acid dependence, the acidity constant K_a for B was found to be 0.08 M compared to a value determined from the immediate spectral changes of A with H^+ of 0.08 M. Several values of k_1 are given in Table V.

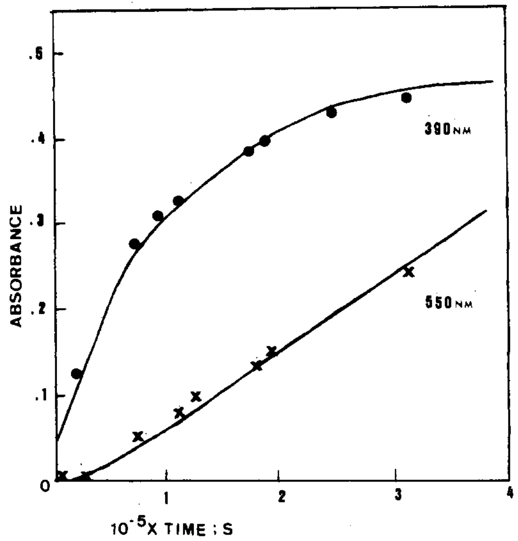

Figure 12. Runge–Kutta fit to experimental data using $k_0 = 3 \times 10^{-8}$ s^{-1}, $k_1 = 0.274$ M^{-1} s^{-1}, and $k_2 = 0.035$ M^{-1} s^{-1} at 25 °C and 0.25 M HCl ($[A]_0 = 3.1 \times 10^{-5}$ M, $[MDA]_0 = 1.54 \times 10^{-5}$ M): (point) experimental determination; (line) Runge–Kutta calculation.

The intermediate I, isolated by benzene extraction of solutions containing mostly I, was used to study its rate of reaction with B to form C. The rate equation followed was $d[C]/dt = k_2[I][B]$. Again only B, not A, was the reactive species and the acidity constant for B could be evaluated from the rate data and was in reasonable agreement with that obtained by the other two methods. Evaluation of k_2 required an extinction coefficient for I, which was obtained by reacting A with excess MDA, assuming complete formation of I, and measuring its solution spectra. Some values of k_2 are given in Table V.

Clearly the rate constants for the reaction of MDA with B are much larger than the rate of hydrolysis of B or the rate of production of C from B in acid media. Also $k_2 < k_1$ by a relatively small factor and both k_1 and k_2 for MMDA are approximately 6× smaller than for MDA.

In order to check and compare the rate constants determined from the MDA–A reaction with the kinetic data from the reaction of A with acid alone, Runge–Kutta calculations were made under both conditions in which the spectral changes expected for these reactions were determined:

$$A + H^+ \overset{K_a}{\rightleftharpoons} B$$

$$B \xrightarrow{k_0} [Ni((AO)_2\text{-}H)]^+ + MDA$$

$$MDA + B \xrightarrow{k_1} I$$

$$I + B \xrightarrow{k_2} C$$

We utilized average values of k_0, k_1, k_2, and K_a, the extinction coefficients, and the light absorption changes with time at two wavelengths. The value of k_0 was estimated (a) from the deviations from the Runge–Kutta values when the k_0 term was not used and (b) from the linear portion of the steady-state formation of C when MDA was not added. The fit at two wavelengths is given in Figure 12 with use of 5×10^{-8} s^{-1} for k_0. The agreement is reasonable in view of the range of experiments they had to fit. Thus our model fits all aspects of known behavior of the system and its major details are no doubt correct. In line with this is the Runge–Kutta calculation of the fit to the MMDA–A spectral-kinetic data, which also was well reproduced by utilizing the rate constants and extinction coefficients determined.

Summary

$[Ni((PnAO)\text{-}6H)]^0$ (A) is a heterocyclic aromatic complex that protonates at the oxime group reversibly in acid media with K_a = 0.08 M at 25 °C, without breaking the intermolecular hydrogen bond (B). With longer reaction times or at higher temperatures hydrolysis occurs, producing malondialdehyde, which condenses with the remaining A in two observable steps to form an intermediate (I) and subsequently C, a condensed dimer. k_0 for this process was estimated to be 3×10^{-8} s^{-1} at 25 °C. Direct reaction of malondialdehyde with A produces the same material (C), and 2-methylmalondialdehyde gives an analogue. The reaction of MDA with A in acid media follows the rate law $d[I]/dt = k_1[MDA][B]$ with $k_1 = 0.28$ M^{-1} s^{-1}, while the second reaction has the analogous rate law $d[C]/dt = k_2[I][B]$, $k_2 = 0.035$ M^{-1} s^{-1} at 25 °C. The UV–visible spectral properties and X-ray single-crystal structures are given for A–C, and some of the properties of I are also determined.

The heterocyclic aromatic ring has a high electron density at the C12 position and is quite reactive to aldehydes in general, including HCHO, CH_3CHO, CF_3CHO, and C_6H_5CHO, usually producing a C12-monosubstituted complex ion. The kinetic studies are to be presented in greater detail in a later paper.[20]

Acknowledgment. We wish to express our appreciation to Dr. E. G. Vassian for initial samples of $[Ni((PnAO)\text{-}6H)]^0$ and to Drs. C. W. Gehrke and Kim Kuo for measuring the spectra of the intermediate I. The NT-300 NMR spectrometer and the CAD4 X-ray diffractometer were purchased partially through NSF Grants DCM-8115599 and CHE-78-20347. Partial support from the Research Council (UMC) and the NSF (Grant CHE-81-06795) is also appreciated.

Registry No. MDA, 542-78-9; MMDA, 16002-19-0; PnAO, 97466-94-9; $[Ni((PnAO)\text{-}6H)]^0$, 18195-22-7; $[Ni((PnAO)\text{-}5H)]^+ClO_4^-$, 69681-23-8; $[Ni((PnAO)\text{-}7H)_2(CH)_3]^+NO_3^-\cdot 2H_2O$, 97466-93-8; $[Ni((PnAO)\text{-}7H)_2(CHC(CH_3)CH)]^+$, 97466-95-0; $[Ni((PnAO)\text{-}6H)CHCHCHO]$, 97466-96-1; $[Ni((PnAO)\text{-}6H)CHC(CH_3)CHO]$, 97466-97-2; 3,3′-[[(2-formylvinyl)-1,3-propanediylidene]dinitrilo]bis[3-methyl-2-butanone oxime], 97466-98-3; 3,3′-[[(2-formylpropenyl)-1,3-propanediylidene]dinitrilo]bis[3-methyl-2-butanone oxime], 97466-99-4.

Supplementary Material Available: Listings of hydrogen atom positions, complete listings of bond distances and angles, and tables of root-mean-square amplitudes of vibration, general temperature factor expressions, and observed and calculated structure factors for compounds A and B and listings of hydrogen atom positions, root-mean-square amplitudes of vibration, and observed and calculated structure factors for compound C (48 pages). Ordering information is given on any current masthead page.

---

(20) Ghiron, A. M.S. Thesis, University of Missouri, Columbia, MO, 1985.

Contribution from the Departments of Chemistry, Chapman College,
Orange, California 92666, and University of Washington, Seattle, Washington 98195

Reducing Properties of Potassium Silyl

VICTOR A. WILLIAMS* and DAVID M. RITTER

Received June 25, 1984

Potassium silyl has been found to act preferentially as a powerful reducing agent rather than as a nucleophilic substitution agent. Reactions with phosphorus trichloride and dimethylchlorophosphine gave polymers containing phosphorus–hydrogen bonds. Trimethylchlorosilane underwent transmetalation with its complicated consequences; carbon dioxide was reduced to carbon monoxide and potassium formate, and nitrous oxide gave nitrogen. Silane and polymeric silicon hydrides were produced in all reactions. Titration of potassium silyl with carbon dioxide showed that the reaction is stepwise and complex.

The earliest reactions of potassium silyl[1,2] ($KSiH_3$) were those of a nucleophile reacting with methyl chloride to give methylsilane quantitatively. A similar reaction with bromodeuteriosilane[2] was incomplete (43% of bromosilane recovered), exhibiting only slightly a nucleophilic displacement (3.4% deuterated disilanes formed) and being instead largely reductive (84% deuteriosilanes formed). These results led to the experiments reported here. The inquiry concerned whether the silyl anion had the properties of a nucleophile, as found for germyl and methyl anions, or behaved as a reducing agent in the manner of the complex hydrido anions of aluminum and boron. The substances considered as reactants were phosphorus trichloride, dimethylchlorophosphine, triethylamine–chloroborane, trimethylchlorosilane, carbon dioxide, nitrous oxide, and nitric oxide.

Experimental Section

Potassium silyl ($KSiH_3$) was prepared by the method of Ring and Ritter.[2] The method was modified slightly according to Ring et al.[3] The use of potassium sand greatly shortened the time needed for the preparation. Potassium sand was prepared according to Hershberg and Fieser.[4] The sand was poured directly into the reaction vessel, and after removal of the toluene, dry monoglyme and silane were added. Reaction was complete in 7–10 days.

After filtration, the potassium silyl solution was kept under dry nitrogen in a vessel equipped with a rubber septum. Transfers were made with a syringe. Solutions were standardized in a variety of ways. Base hydrolysis and measurement of the liberated hydrogen, reaction with gaseous hydrogen chloride to produce silane, silicon colorimetric analysis,[5] and gravimetric potassium analysis[6] gave reproducible and self-consistent results. The range of concentration of solutions prepared in this manner was typically from 0.3 to 0.7 M. The titer did not change over a period of several months. Reactions were carried out by introducing solutions

Table I. Reaction with Volatile Oxides[a]

	CO_2	N_2O	NO
	Reactants		
$KSiH_3$ in	1.4	0.90	1.14
gas in	4.96	5.4	4.6
gas out	2.04	3.8	0.135
gas consumed	2.92	1.6	4.5
	Gaseous Product		
SiH_4	0.67	0.21	0.163
other gases	1.46 (CO)	2.15 ($N_2 + H_2$)	1.18 (N_2O) 2.0 ($N_2 + H_2$)
	Solid Product		
K found	1.45		
H_2 from basic hydrolysis	0.41	0.78	1.03
Si in residue	0.9	0.8	

[a] All amounts in mmol.

---

* To whom correspondence should be addressed at Chapman College.

(1) Sampson Isenberg, Doctoral Dissertation, University of Chicago, 1937.
(2) M. A. Ring and D. M. Ritter, *J. Am. Chem. Soc.*, **83**, 802 (1961).
(3) R. C. Kennedy, L. P. Freeman, A. P. Fox, and M. A. Ring, *J. Inorg. Nucl. Chem.*, **28**, 1373 (1966).
(4) E. B. Hershberg and L. F. Fieser, *Org. Synth.*, **18**, 225 (1938).
(5) A. Ringborn, P. E. Ahlers, and S. Siitonen, *Anal. Chim. Acta*, **20**, 78 (1959).
(6) J. Kohler, *Fresenius' Z. Anal. Chem.*, **138**, 9 (1952).

0020-1669/85/1324-3278$01.50/0